Results from Sudden Loss of Vacuum on Scaled Superconducting Radio Frequency Cryomodule Experiment

Andrew A. Dalesandro[a], Ram C. Dhuley[b], Jay C. Theilacker[a], and Steven W. Van Sciver[b]

[a]*Fermi National Accelerator Laboratory, P.O. Box 500, Batavia, IL 60510 USA*
[b]*National High Magnetic Field Laboratory, Tallahassee, FL 32310 USA*

Abstract. Superconducting radio frequency (SRF) cavities for particle accelerators are at risk of failure due to sudden loss of vacuum (SLV) adjacent to liquid helium (LHe) spaces. To better understand this failure mode and its associated risks an experiment is designed to test the longitudinal effects of SLV within the beam tube of a scaled SRF cryomodule that has considerable length relative to beam tube cross section. The scaled cryomodule consists of six individual SRF cavities each roughly 350 mm long, initially cooled to 2 K by a superfluid helium bath and a beam tube pumped to vacuum. A fast-acting solenoid valve is used to simulate SLV on the beam tube, from which point it takes over 3 s for the beam tube pressure to equalize with atmosphere, and 30 s for the helium space to reach the relief pressure of 4 bara. A SLV longitudinal effect in the beam tube is evident in both pressure and temperature data, but interestingly the temperatures responds more quickly to SLV than do the pressures. It takes 500 ms (roughly 100 ms per cavity) for the far end of the 2 m long beam tube to respond to a pressure increase compared to 300 ms for temperature (approximately 50 ms per cavity). The paper expands upon these and other results to better understand the longitudinal effect for SRF cryomodules due to SLV.

Keywords: Loss of Insulating Vacuum, Condensation Heat Transfer, Superconducting RF.

INTRODUCTION

One of the next generation experiment proposals at Fermilab is the Project X linear accelerator which utilizes approximately 30 SRF cryomodules to accelerate charged particles to nearly the speed of light. The SRF cavities which comprise these cryomodules are held at temperatures in the range of 1.8 to 2.0 K by baths of superfluid helium (He II) to maintain superconductivity. If the cryomodule insulating vacuum or beam tube vacuum experience a rupture to atmosphere, the resulting ambient air inflows into evacuated spaces of LHe-cooled cavities produce rapid air condensation on the cold walls of the cavities. The rapid air condensation is the result of significant heat transfer between the inflowing air and the LHe used to cool the cavities, resulting in rapid vaporization and pressurization of the LHe containment vessels within the cryomodule. SLV is often considered the worst-case failure scenario in the design of large cryogenic systems. Specifically SLV of accelerating particle beam tubes has been shown on average to be worse than SLV of the space surrounding a LHe vessel, the insulating vacuum, due to the impedance of radiation shields, magnetic shields and/or multi-layer insulation (MLI) [1,2]. The rapid condensation of air resulting from SLV in cryogenic systems holds down the air vapor pressure, maintaining the pressure in the ruptured vessel relatively low, thus allowing more air molecules to enter the low pressure environment (and further contribute to the condensation rate), than would be expected in a room temperature SLV failure. This effect is known as cryopumping because the cryogenically cooled surfaces driving the condensation act to lower the pressure significantly more than what would normally exist in a room temperature vacuum with a comparable number of air molecules.

Because heat transfer via air condensation is largely dependent on incoming air flow cross section and condensation surface area, the geometry of a system plays an important role when considering the effects of SLV failure. Previous work on SLV failure in SRF systems has focused on quantifying the heat flux from air condensation on the LHe vessel(s), with mean heat fluxes largely on the order of 1 - 4 $W*cm^{-2}$ [1-4]. Most relevant to the present experiment is a SLV failure experiment performed by the German Electron-Synchrotron (DESY) of a XFEL cryomodule consisting of 1.3 GHz elliptical cavities similar to what is proposed for Project X. In this test DESY measured a mean heat flux from beam line SLV failure of 2.3 $W*cm^{-2}$, as well as a time delay in the pressure propagation from vacuum failure of 4 s along the 12 m long cryomodule beam length [1]. This paper presents the

design of an experiment with a high aspect ratio, or considerable axial length and LHe cooled surface area relative to beam tube cross section to observe the longitudinal effect observed by the DESY XFEL during SLV and present data to help characterize the effect [5].

THE EXPERIMENT

The experiment is designed to simulate SLV failure for a scaled Project-X style SRF cryomodule, and consists of six 1 L LHe cavities connected by a 25 mm diameter riser pipe to a common 100 mm diameter helium gas (GHe) header. Passing through the six LHe vessels is a common 25 mm diameter evacuated beam tube spanning the 2 m length of the experiment. A diagram of the experimental setup is shown in Figure 1. To capture the longitudinal effect of SLV in the beam tube, absolute pressure measurements are recorded along the axial length at increments of approximately 350 mm (see Table 2 for more details) using Validyne differential pressure variable reluctance transmitters, referenced to cryostat vacuum, nominally 10^{-9} mbar. In addition, temperatures are recorded at similar intervals along the length of the beam tube on the vacuum (failure) side as well as the LHe side using Lakeshore Cernox CX-1050 RTDs, bonded by Stycast to the experiment. The entirety of the experiment is constructed of 304 stainless steel, for ease of fabrication and to limit axial conduction between cavities. Pressure and temperature transmitters are also located on the LHe and GHe circuits as shown in Figure 1. Differential pressures are measured on the external orifice flow meter on the inlet to the beam tube vacuum space and on the exit of the GHe header upstream of the 4 bara helium relief. Liquid level measurements are collected by AMI superconducting level probes in the 25 mm riser pipes of cavity one and cavity six. This experiment was conducted at the National High Magnetic Field Laboratory at Florida State University in the CHEF cryostat [5]. Table 1 lists some of the important initial conditions of the experiment just prior to simulation of SLV using the 25 mm solenoid valve.

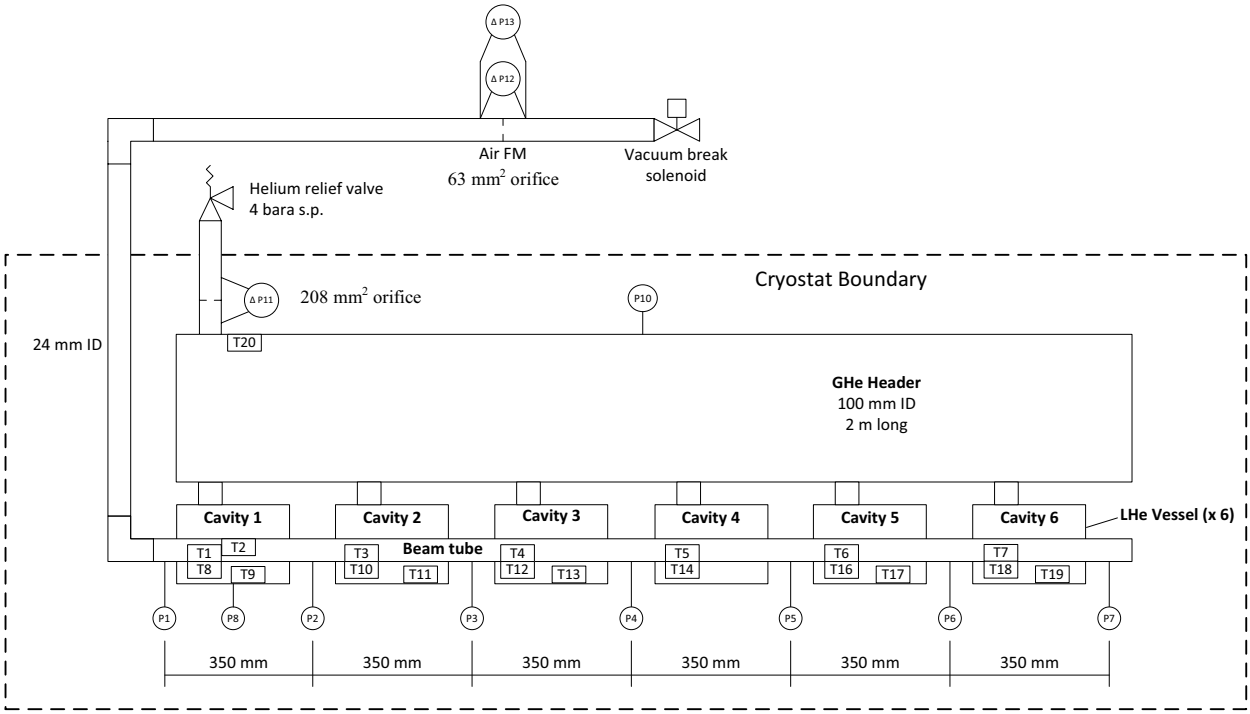

FIGURE 1. SLV Experiment Schematic.

TABLE 1. SLV Experiment Initial Conditions

Variable	Value	Units
LHe bath temperature	2.0	K
LHe bath pressure	3129	Pa
Initial beam tube pressure	10^{-5}	mbar
Beam tube cold surface area	1357	cm^2
Initial LHe volume	8.2	L
Total GHe volume	17.5	L

RESULTS

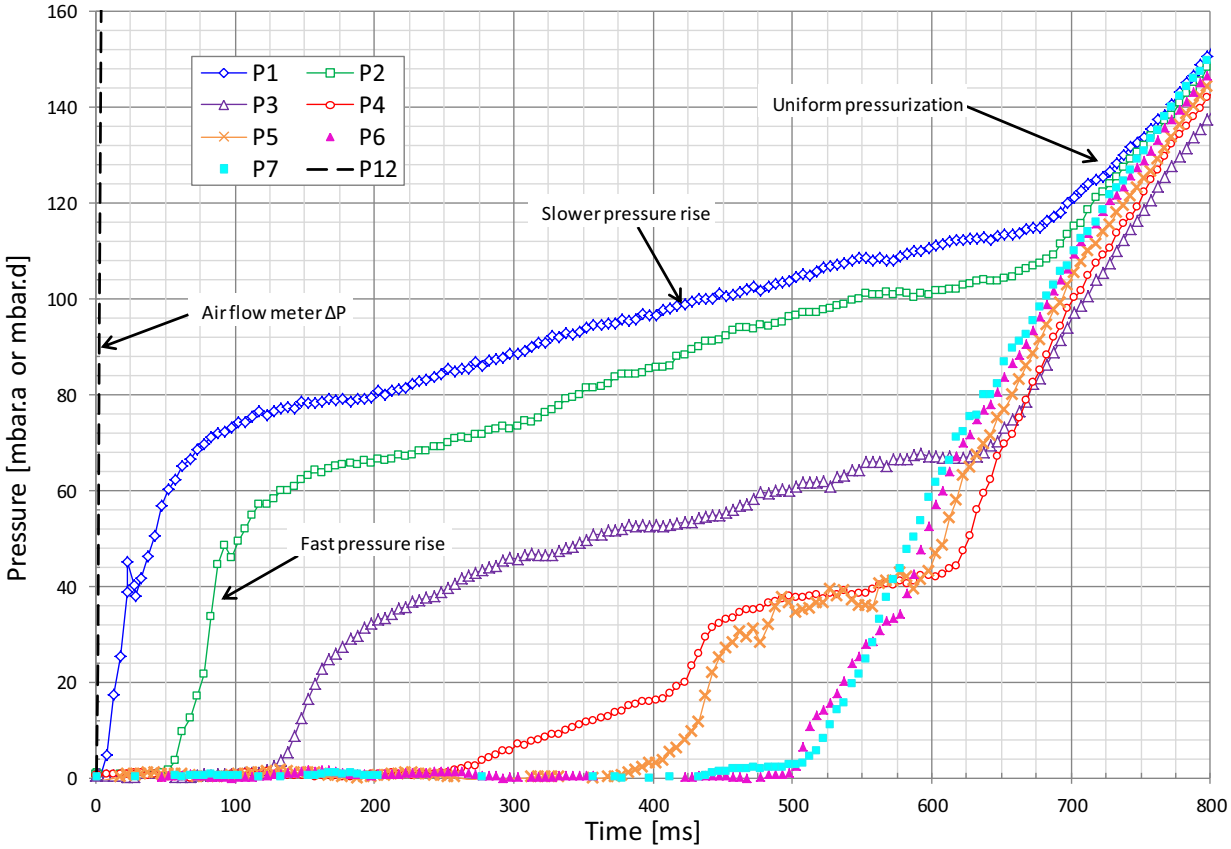

FIGURE 2. Beam Tube Pressure Profile 800 ms following SLV

Figure 2 shows the pressurization profile of the beam tube vacuum rupture for 800 ms immediately following SLV, where P1 (diamonds with line) and P7 (squares with no line) are the transmitters on the near and far ends of the cryomodule, respectively. Also included is a small portion of the differential pressure measured across the air orifice upstream of the beam tube (dashed line along the vertical axis) shown to reference the onset of SLV. One of many interesting features of this plot is the time delay between the initial pressure spike recorded by P1 at cavity one, the first cavity to experience the incoming atmospheric air, and each subsequent pressure transmitter axially along the length of the beam. Table 2 lists the timing of the initial pressure spikes recorded by each transmitter, that transmitter's axial displacement from P1 along the beam tube and the average air pressure propagation velocity to

each transmitter downstream of P1. It takes over 500 ms for P7, after cavity six, to record the incident pressure spike first recorded by P1. The average pressure propagation velocity in the beam tube generally decreases with axial distance from the beam tube inlet from about 7.0 $m*s^{-1}$ at P2 to 4 $m*s^{-1}$ at P7; this is several orders of magnitude lower than the speed of sound for air at atmospheric conditions. This average pressure propagation velocity is consistent with results from the DESY XFEL cryomodule crash test which had a 4 s delay along the length of a 12 m long cryomodule for an average pressure propagation velocity of approximately 3.0 $m*s^{-1}$ [1]. This slow pressure propagation is evidence of the longitudinal effect in strings of SRF cavities which have considerable cold length and surface area relative to vacuum venting cross section.

TABLE 2. Beam tube pressure propagation time delays, distances and average air pressure propagation velocity along beam tube axis after SLV

Sensor	initial pressure spike after SLV	Δtime between pressure spikes	distance from P1	avg. velocity of pressure spike propagation	time until uniform pressurization rate
P1	7 ms		-	-	732 ms
P2	57 ms	50 ms	349 mm	7.0 m/s	692 ms
P3	132 ms	75 ms	691 mm	5.5 m/s	632 ms
P4	277 ms	145 ms	1037 mm	3.8 m/s	602 ms
P5	407 ms	130 ms	1384 mm	3.5 m/s	587 ms
P6	507 ms	100 ms	1730 mm	3.5 m/s	507 ms
P7	512 ms	5 ms	2120 mm	4.2 m/s	512 ms

The slow pressure propagation velocity is the result of all the air molecules entering a cavity being successfully cryopumped by the 2 K inner surface of the cavity during the first 10-100 ms of exposure to each cavity along the length of the cryomodule. This cryopumping is driven by the condensation rate within a given cavity and is a function of two separate components. One is the condensation capacity of a given cavity, which is the maximum amount of energy a cavity is capable of extracting from the inflow of air molecules, and is itself a function of the impedance of the cavity cold surface area (which increases with condensation layer thickness) and the heat capacity of the cavity walls, which is largely dependent on the phase of the helium (He II is highest, supercritical helium is lowest). For simplicity the condensation capacity can be thought of as the number of air molecules a cavity is capable of condensing. The other component of the condensation rate is the amount of energy flux into a cavity, which is equal to the number of air molecules entering a cavity times the enthalpy of those molecules. For simplicity the amount of energy entering a cavity can also be thought of as the incoming air flow rate to a given cavity in terms of a number of molecules. As the first warm air molecules enter a previously unaffected cavity the condensation rate ramps rapidly until peaking. The peak condensation rate within a cavity cannot exceed the flow of air into the cavity, and is likely smaller than the peak air flow rate. Eventually the air flow rate into the cavity exceeds the condensation rate and the remaining molecules are cryopumped to the next cavity downstream. This process repeats for all remaining cavities downstream.

Table 2 also shows the change in the time delay between pressure spikes. The time between the pressure spikes grows at first, from 50 ms between P1 and P2, to 145 ms between P3 and P4, and then decays to just 5 ms between P6 and P7. The growth in the time delay is likely due to the small number of air molecules that first enter a downstream cavity and the likely pre-cooling that these molecules experience by moving through a partially cold upstream cavity. This pre-cooling in upstream cavities helps to reduce the amount of energy required for condensation in downstream cavities, up to P4 (cavity three) at 145 ms after SLV. After P4 this time delay starts shrinking again, which is harder to explain but could be the result of degradation in the pre-cooling effect and/or an effective pre-warming of downstream cavities prior to pressure propagation to those cavities as a result of downstream condensation (see discussion on temperature propagation before Figure 4).

For cavities one through four, after the initial pressure spike and fast pressurization rate there is a slower intermediate pressurization rate with a more horizontal slope than at the initial pressure spike. This intermediate, slower pressurization rate can be thought of as a period of downstream condensation. Even as air inflows into the beam tube persist at fairly constant rates for the first 600 ms after SLV (see Figure 3), the pressurization rates along the beam tube vary significantly during this time period. The inflow of air into cavity one causes its pressure to rise rapidly for the first 60 ms after SLV, and then the pressurization rate slows considerably until about 732 ms after

SLV when the pressurization rate ramps up again, matching the pressurization rate in all of the cavities (see discussion on uniform pressurization after Figure 3). Cavity six is the only cavity not to experience an intermediate, slower pressurization rate, because once the condensation rate in cavity six declines, there is no more downstream condensation, and all uncondensed particles work to pressurize the cavity. This is also why P6 and P7 have remarkably similar pressure profiles.

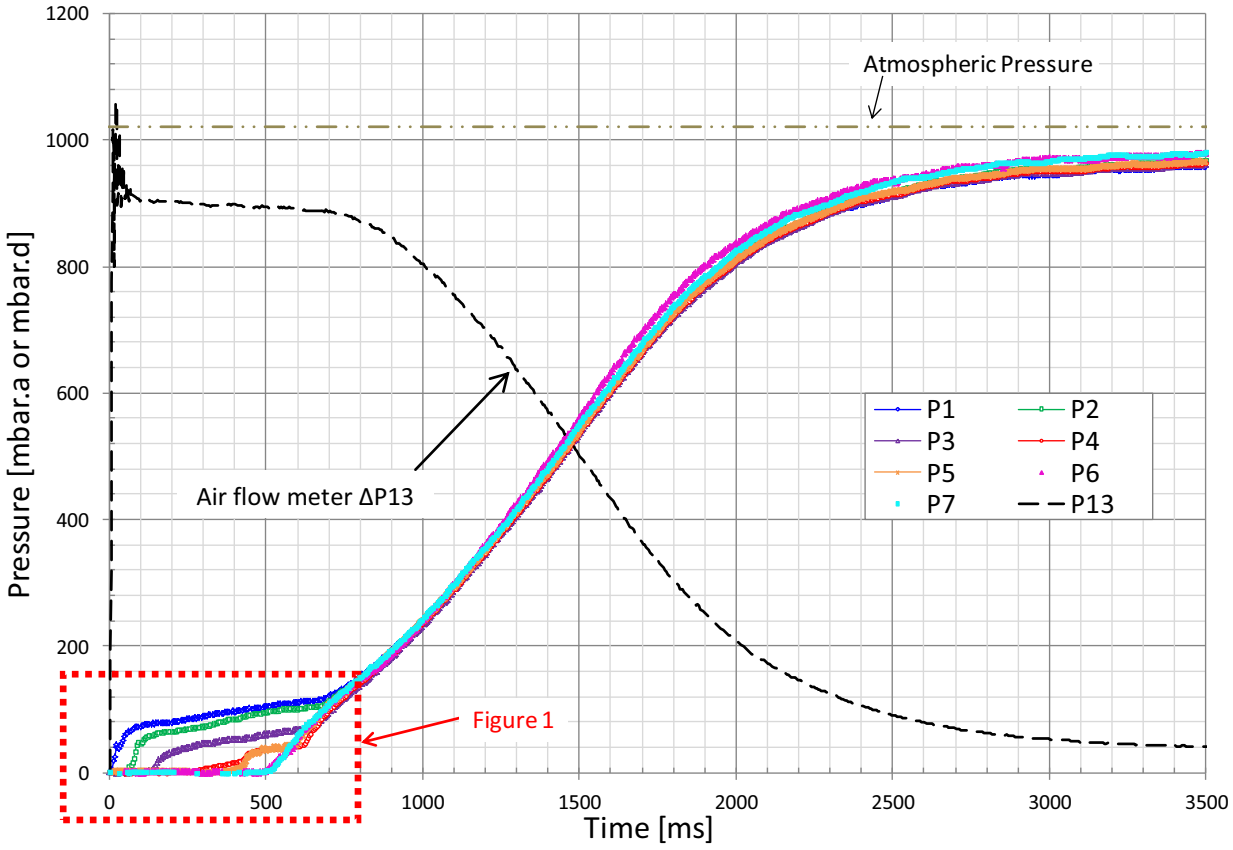

FIGURE 3. Beam Tube Pressure Profile 3500 ms following SLV

Another interesting characteristic of the pressurization profile in Figure 2 and Figure 3 is the period of uniform pressurization across all cavities in the cryomodule beam tube, which is visible at around 700 ms after SLV. Uniform pressurization occurs once cryopumping in the beam tube stops, because at this point the beam tube is still well below atmospheric pressure. For the same reason that cavity six does not experience an intermediate, slower pressurization rate, it also starts the period of post-condensation pressurization when the initial pressure spikes of P6 and P7 occur around 500 ms after SLV. Accordingly cavity one is the last to join in the uniform pressurization which begins at about 732 ms after SLV until the beam tube internal pressure is equalized to atmosphere, which it starts approaching asymptotically around 3000 ms after SLV.

Figure 4 shows the temperature profile on the inner surface of the cryomodule axially along the beam line. Thermometers are spaced comparably to the pressure transmitters in the experiment (see Figure 1 for orientation of thermometers and Table 3 for specific dimensions and temperature spike propagation velocities). Of note for Figure 4 is that the temperature data from this experiment is particularly noisy and largely unreliable quantitatively, therefore is only discussed for trending. Although the axial displacement between thermometers is comparable to that of the pressure transmitters, comparing Figure 2 and Figure 4 it is evident that the timing of the temperature spikes in Figure 4 do not coincide with those of the pressure spikes seen in Figure 2. This shorter time delay between temperature spikes results in a faster temperature propagation velocity, which decreases with axial displacement as shown in Table 3. The reason that the temperature profile has a higher propagation velocity is likely

because cryopumping of air molecules in downstream cavities helps to maintain the vapor pressure of the molecules to a level below the resolution limits of the pressure transmitters, while heat is transferred to the walls of the cavity, where the thermometers are mounted. The time delay between the temperature and pressure spikes in a given cavity is the period of increasing condensation rates in the cavities due to cryopumping. The result is a longitudinal temperature propagation delay of only 300 ms and a longitudinal pressure propagation delay of 500 ms.

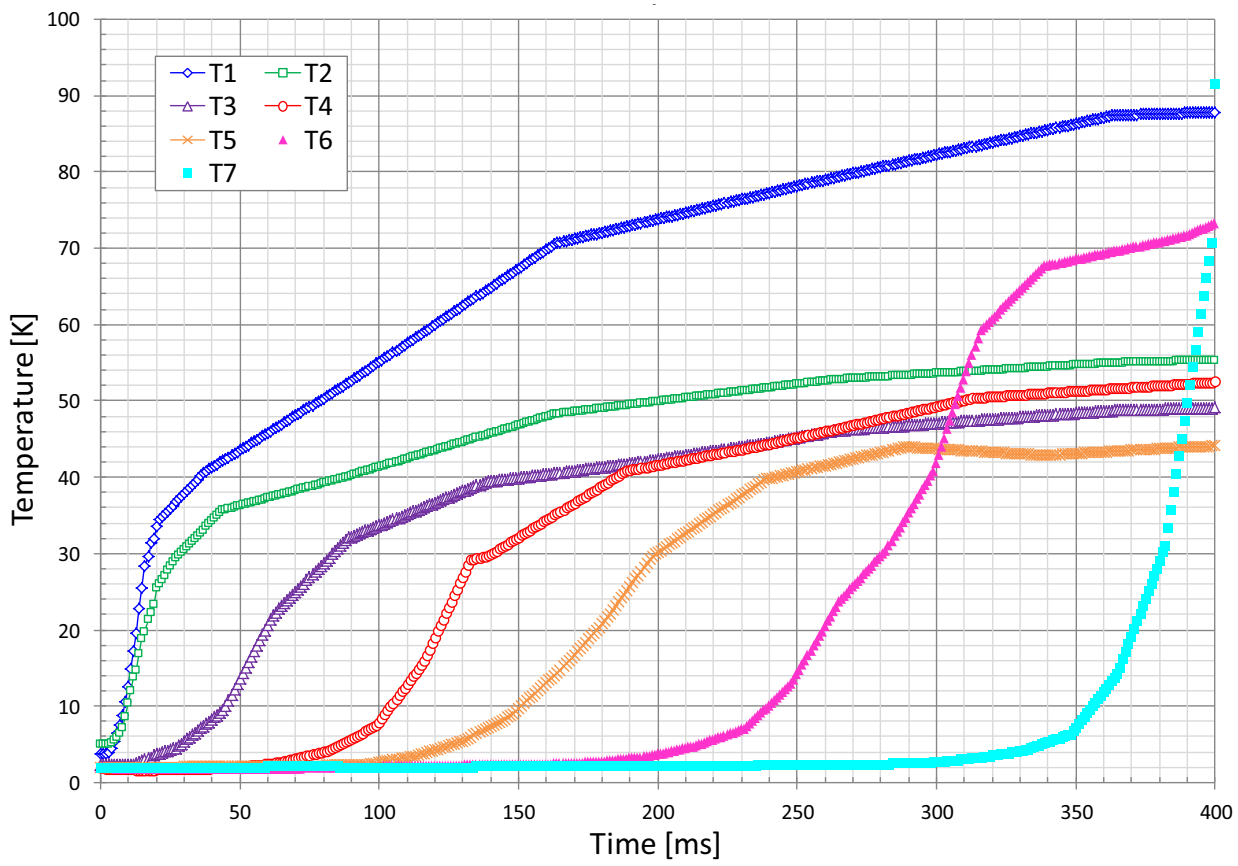

FIGURE 4. Beam Tube Temperature Profile 400 ms following SLV

TABLE (3). Beam tube temperature propagation time delays, distances and average air temperature propagation velocity along beam tube axis after SLV. Note that temperature sensor T2 is located at the same axial displacement as T1 within the beam tube, with a 180° radial offset from T1.

Sensor	initial temperature spike after SLV	Δtime between temperature spikes	distance from T1	avg. velocity of temperature spike propagation
T1	3 ms		-	-
T2	5 ms		-	-
T3	12 ms	9 ms	346 mm	38.5 m/s
T4	49 ms	37 ms	692 mm	15.0 m/s
T5	97 ms	48 ms	1038 mm	11.0 m/s
T6	181 ms	84 ms	1384 mm	7.8 m/s
T7	298 ms	117 ms	1730 mm	5.9 m/s

Another observation from Figure 4 and shown in Table 3 is an increasing time delay between temperature spikes as the air propagates to downstream cavities, similar to the increasing pressure propagation discussed above. However, unlike the pressure propagation delay which only increases initially and then decreases near the end of the beam line, the temperature propagation time delay only ever increases, from 9 ms between T1 and T3 to 117 ms between T6 and T7. The reasons speculated for the reversal in the pressure propagation delay are a possible degradation in the pre-cooling effect from upstream cavities and/or a pre-warming effect to downstream cavities as a result of cryopumping. These reasons can be consistent with a steady increase in the temperature propagation delay because of the timing differences between temperature and pressure propagation. The pressure propagation delay reversal occurs between the pressure spikes for P4 at 277 ms and P5 at 407 ms (see Table 2), which overlaps the time for the temperature propagation to reach all six cavities of 298 ms. The temperature propagation spikes mark the onset of downstream cryopumping (pre-warming of cavities downstream) and once the temperature propagation reaches cavity six at 298 ms after SLV, the pre-cooling of molecules can only degrade with time.

CONCLUSION

The SLV experiment shows a clear longitudinal effect along the beam tube axis for the first 700 ms. Comparing this longitudinal effect to other literature it appears that the effect is not unique to this experiment and is scalable to other systems of similar geometries [1]. The longitudinal effect resulting from SLV in SRF beam lines is a result of the high aspect ratio of cold surface area to rupture flow cross section. Each cavity in series experiences a brief period of cryopumping, resulting in aggregate in a prolonged period of cryopumping down the length of the particle beam line, which is visible by the propagation delay in pressure for the first 500 ms and temperature for the first 300 ms along the length of the beam tube. When cryopumping stops propagating downstream around 500 ms, the result is a propagating pressurization back upstream until the entire beam line is increasing in pressure uniformly around 700 ms until equalizing with atmosphere around 3000 ms, which lasts through the duration of the experiment.

ACKNOWLEDGMENTS

Fermilab is operated by Fermi Research Alliance, LLC under Contract No. DE-AC02-07CH11359 with the United States Department of Energy. Thanks to Ernesto Bosque, Mark Vanderlaan, Joe Brown, Wayne Johnson, Steve Cullum, and James O'Neill for technical assistance.

REFERENCES

1. T. Boeckman et al, "Experimental Tests of Fault Conditions During the Cryogenic Operation of a XFEL Prototype Cryomodule," Proceedings of International Cryogenic Engineering Conference 22 - International Cryogenic Materials Conference 2008, H. M. Chang et al, Seoul, 2009.
2. W. Lehmann and G. Zahn, "Safety Aspects for LHe Cryostats and LHe Transport Containers," Proceedings of International Cryogenic Engineering Conference 7, London, 1978.
3. S. M. Harrison, "Loss of Vacuum Experiments on a Superfluid Helium Vessel," in IEEE Transactions on Applied Superconductivity, Vol. 12, No.1, March 2002
4. M. Wiseman et al, "Loss of Cavity Vacuum Experiment at CEBAF," *Advances in Cryogenic Engineering 39*, edited by P. Kittel, Plenum Press, New York, 1994, pp. 997-1003.
5. A. A. Dalesandro, J. Theilacker, S. W. Van Sciver, "Experiment for transient effects of sudden loss of vacuum on a scaled superconducting radio frequency cavity," AIP Conference Proceedings 1434, American Institute of Physics, Melville, NY, 2012, pp. 1567-1574.